

Spin-Coupled Valence Bond Study of the Reaction between Benzene and a Methyl Cation

Guido Raos*

Dipartimento di Chimica, Politecnico di Milano, via Mancinelli 7, 20131 Milano, Italy

Luca Astorri and Mario Raimondi

Dipartimento di Chimica Fisica ed Elettrochimica, Università di Milano, and Centro CNR CSRSRC, via Golgi 19, 20133 Milano, Italy

David L. Cooper

Department of Chemistry, University of Liverpool, P.O. Box 147, Liverpool, U.K. L69 3BX

Joseph Gerratt

School of Chemistry, University of Bristol, Cantocks Close, Bristol, U.K. BS8 1TS

Peter B. Karadakov

Department of Chemistry, University of Surrey, Guildford, Surrey, U.K. GU2 5XH

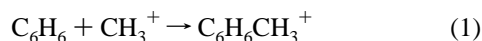
Received: September 25, 1996; In Final Form: January 15, 1997[⊗]

We present spin-coupled valence bond calculations on the reaction pathway for the insertion of a methyl cation onto the aromatic system of benzene, leading to the Wheland intermediate $C_6H_6CH_3^+$. Simultaneously with the geometrical rehybridization of the two carbons forming the new substrate-electrophile bond (from sp^2 to sp^3), we observe the crossing of two spin-coupled potential energy curves; at large separations, these correspond to $C_6H_6 + CH_3^+$ and to $C_6H_6^+ + CH_3$. In the neighborhood of the crossing point, the spin-coupled valence bond wave function obtained by mixing these two orbital configurations switches continuously from the former to the latter.

Introduction

In a recent publication¹ we applied spin-coupled (SC) theory² to the study of the electronic structure of the σ complexes, or Wheland intermediates, formed by addition of a proton to benzene, phenol, and benzonitrile. Their energies were shown to correlate well with the activating/deactivating and the *ortho/meta/para* directing character of the substituents. Furthermore, we found that their SC wave functions could be readily interpreted in terms of valence bond (VB) resonance structures. In summary, we provided *ab initio* support for the qualitative VB arguments that are used in any organic chemistry textbook for the discussion of the energetics and selectivity of aromatic electrophilic substitution reactions.³

In this paper we present an account of our SC calculations on the reaction pathway for the insertion of the methyl cation, an electrophile, onto the aromatic system of benzene:



The “product” is actually the Wheland intermediate, with a tetrahedral configuration at the site of attack. Of course, reaction 1 is a rather drastic simplification with respect to the actual conditions of electrophilic substitution reactions, as they are commonly carried out in organic chemistry laboratories.³ Nonetheless, even such a simple model system poses some interesting challenges for a modern VB description of the approach of an electron-poor center to the ring, the disruption of the aromatic π conjugation, and the simultaneous formation of a new C–C σ bond. We expect to be able to export much

of the knowledge and understanding acquired here to the study of more complicated and chemically realistic aromatic electrophilic reactions.

In the following section we introduce our computational strategy. Afterward we present our numerical results⁴ and their interpretation. Finally, we summarize our main conclusions and discuss a few general points.

Methods and Calculations

The spin-coupled (SC) and the spin-coupled valence bond (SCVB) methods represent a modern generalization of “classical” VB theory, and they have been extensively reviewed elsewhere.² A short introductory account can also be found in our previous paper.¹ The SC method adopts the most general single-configuration model wave function: the SC orbitals are singly occupied and nonorthogonal, and all possible modes of coupling of the electron spins are explicitly taken into consideration. The shapes of the orbitals and the weights of the different spin couplings are determined simultaneously by minimizing the energy of the SC wave function, as prescribed by the variational principle. We stress that the SC wave function and energy are not invariant to a linear transformation of the orbitals, unlike the ordinary Hartree–Fock case. Thus the analysis of the SC orbitals, which are unique, provides the basis for an objective interpretation of the molecular electronic structure.

A SCVB calculation involves the solution of a nonorthogonal configuration interaction problem, with a “ground state” configuration corresponding to the SC solution and an appropriate set of “excited state” configurations. In this particular case, we shall see that there is a range of nuclear geometries for which

[⊗] Abstract published in *Advance ACS Abstracts*, February 15, 1997.

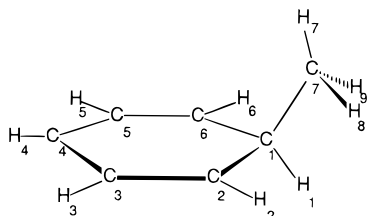


Figure 1. Numbering of the atoms of $C_6H_6 + CH_3^+$.

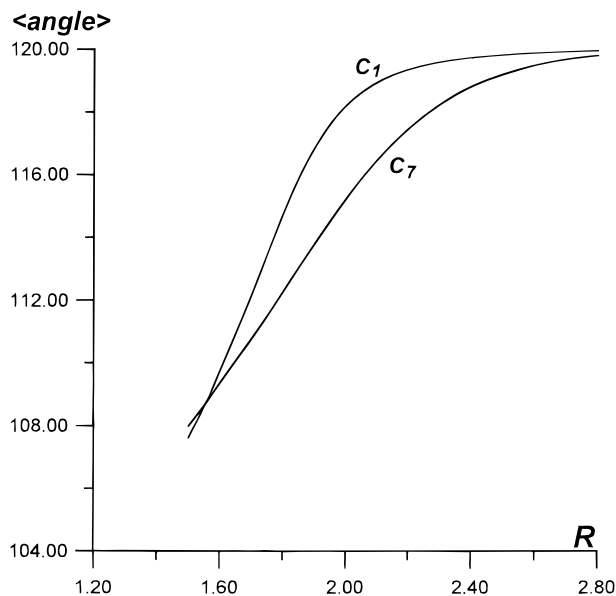


Figure 2. Averages of three bond angles at C_1 ($C_2C_1C_6$, $C_2C_1H_1$, and $C_6C_1H_1$) and at C_7 ($H_7C_7H_8$, $H_7C_7H_9$, and $H_8C_7H_9$), as a function of the C_1-C_7 distance (R , in Å); see Figure 1 for the numbering of the atoms.

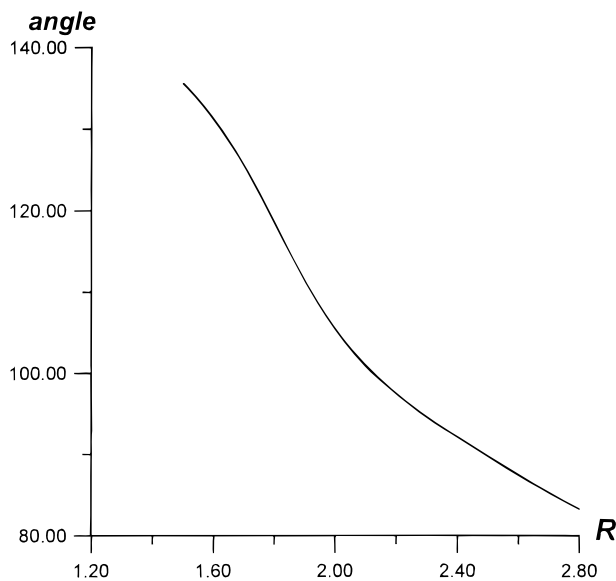


Figure 3. Angle $C_4C_1C_7$ as a function of the C_1-C_7 distance (R , in Å); see Figure 1 for the numbering of the atoms.

two distinct SC solutions are obtained: The two sets of SC orbitals and spin-coupling modes correspond to qualitatively different electron distributions and bonding schemes. The SCVB calculations were carried out by taking a linear combination of these two orbital configurations and solving the resulting secular problem $(\mathbf{H} - E\mathbf{D})\mathbf{c} = 0$, where \mathbf{c} is the vector of the coefficients of the different nonorthogonal structures and \mathbf{H} and \mathbf{D} are the matrices of the Hamiltonian operator and of the overlaps between them.

TABLE 1: Total Energies (in au: $1 E_h = 2625.5$ kJ/mol = 627.5 kcal/mol) of the Reacting Complex, as a Function of the R Coordinate (in Å)

R	E_{RHF}	$E_{SC(1)}$	$E_{SC(2)}^a$	E_{SCVB}
1.50	-270.050 082	-270.102 325		
1.5588	-270.051 644	-270.104 899		
1.60	-270.051 005	-270.104 859		
1.65	-270.048 853	-270.103 299		
1.70	-270.045 654	-270.100 474		
1.75	-270.041 819	-270.096 729	-270.091 747	-270.102 082
1.80	-270.037 682	-270.092 344	-270.087 809	-270.098 273
1.85	-270.033 495	-270.087 651	-270.083 949	-270.094 364
1.90	-270.029 417	-270.082 879	-270.080 358	
1.95	-270.025 524	-270.078 210	-270.077 092	-270.087 078
2.00	-270.021 832	-270.073 779	-270.074 147	-270.083 903
2.05	-270.018 334	-270.069 585	-270.071 463	
2.10	-270.015 010	-270.065 605	-270.068 971	-270.078 279
2.15	-270.011 842	-270.061 852	-270.066 568	
2.20	-270.008 810	-270.058 252	-270.064 209	-270.073 047
2.25	-270.005 899	-270.054 763	-270.061 859	
2.30	-270.003 097	-270.051 411	-270.059 473	-270.067 832
2.35	-270.000 392	-270.048 167	-270.057 083	
2.40	-269.997 777	-270.045 048	-270.054 694	
2.45	-269.995 245	-270.042 017	-270.052 303	-270.059 859
2.50	-269.992 792	-270.039 128	-270.049 922	-270.056 937
2.60	-269.988 113		-270.045 300	
2.70	-269.983 724		-270.041 041	
2.80	-269.979 630		-270.037 484	
2.90	-269.975 832		-270.034 249	
3.00	-269.972 340		-270.031 329	
			-270.031 591*	
4.00	-269.946 692		-270.010 043*	
6.00	-269.937 453		-270.002 097*	
10.0	-269.934 734		-269.999 569*	
50.0	-269.933 783		-269.998 688*	

^a Three spin couplings, except where indicated by the asterisk (*); see also the main text.

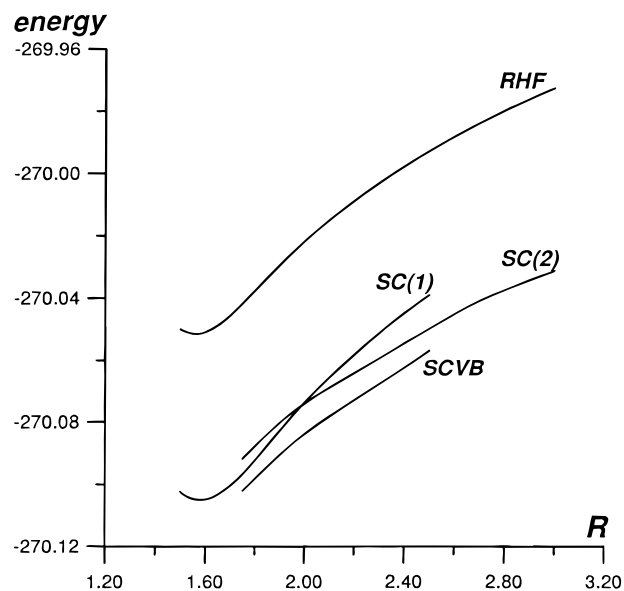


Figure 4. RHF, SC, and SCVB potential energy curves (energies in au, R in Å); see Table 1 for the numerical values.

The system and the numbering of its atoms are illustrated in Figure 1. The reaction coordinate for the insertion of the electrophile corresponds to the distance between the C atom of the methyl group and the aromatic C atom that undergoes the electrophilic attack (*i.e.* C_7 and C_1 in Figure 1). For each C_1-C_7 distance (indicated by R in the following), the geometry of the complex was optimized at the closed-shell restricted Hartree-Fock⁵ (RHF) level of theory using the GAMESS-UK program.⁶ A few constraints were imposed on the geometry optimization: C_s symmetry was assumed throughout (the

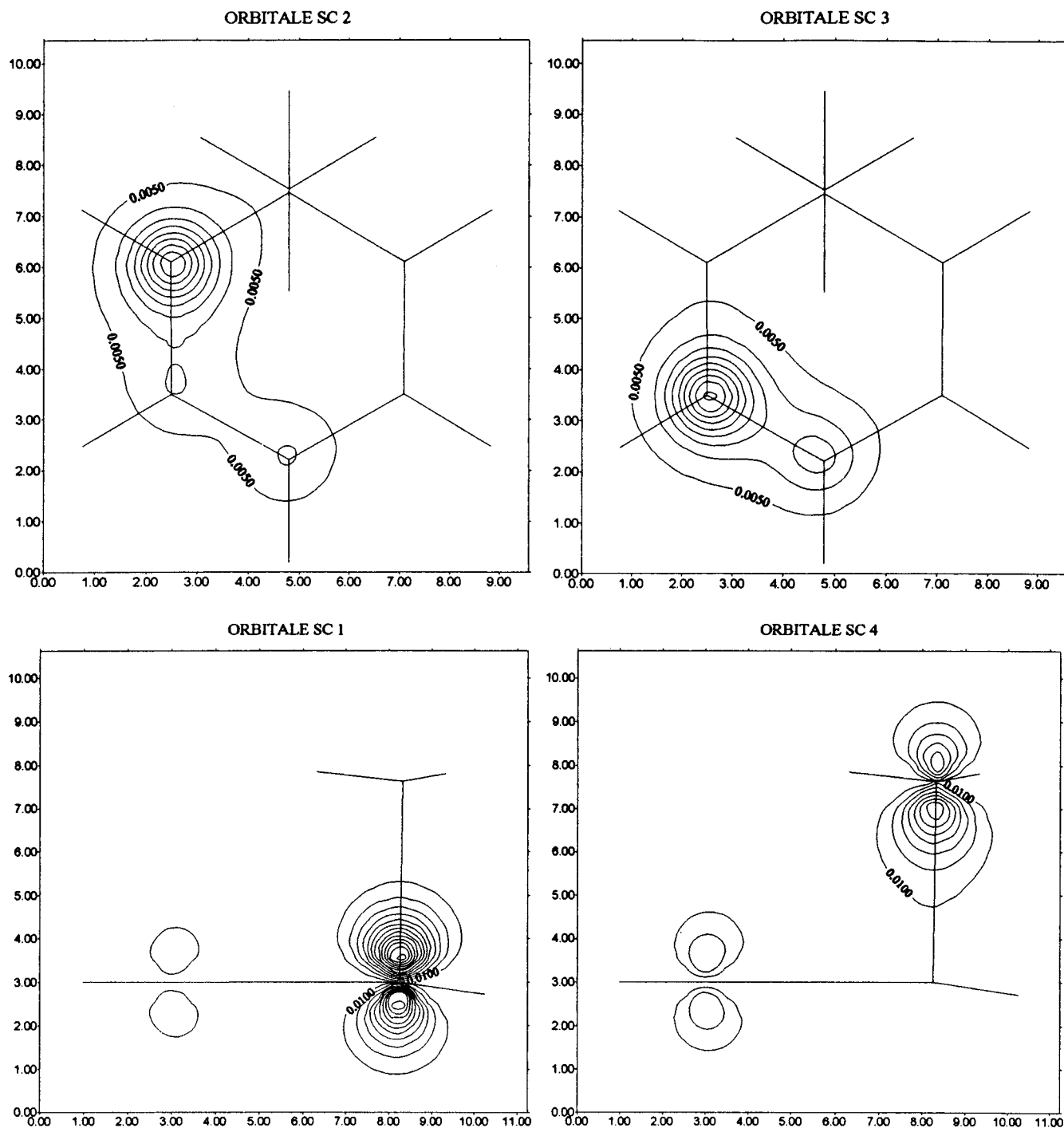


Figure 5. SC(1) solution at $R = 2.45 \text{ \AA}$: contour plots of the square of the orbitals, $|\phi_i(r)|^2$. Orbitals ϕ_2 and ϕ_3 (ϕ_5 and ϕ_6 are symmetric) are plotted in a plane parallel to the benzene ring, shifted by $0.9 \text{ au} = 0.476 \text{ \AA}$ toward the CH_3 group. Orbitals ϕ_1 and ϕ_4 are plotted in the symmetry plane defined by C_4 , C_1 , and C_7 (see Figure 1 for the numbering of the atoms).

symmetry plane passes through C_1 , C_4 , and C_7) and all ring atoms except H_1 were constrained to be coplanar. Care had to be taken in order to avoid convergence of the RHF calculation to an excited state solution, with a reversed ordering of the HOMO/LUMO pair of orbitals. A standard 6-31G* basis set⁵ was used in all calculations.

The SC and SCVB calculations were performed at the optimized RHF geometries. The number of "active" correlated electrons was six: on the reactants side of (1) they correspond to the orbitals of the π system of benzene, whereas on the product side they correspond to the C_1 – C_7 bond and to the four π electrons (actually, quasi- π , since the plane containing the ring is not a symmetry element) characteristic of the Wheland

intermediate.^{1,3} The remaining electrons were kept in a "frozen core" of doubly occupied orbitals, obtained by Pipek–Mezey localization⁷ of the converged RHF orbitals. The spins of the six active electrons are singlet-coupled, so that there are five distinct spin-coupling modes for each orbital configuration.²

Results and Discussion

At the RHF level, the minimum-energy equilibrium geometry is found at $R = 1.5588 \text{ \AA}$. Figures 2 and 3 represent the variation of the most significant structural features of the reacting complex as a function of the C_1 – C_7 internuclear distance, namely, the average bond angles at C_1 and C_7 (Figure 2; see

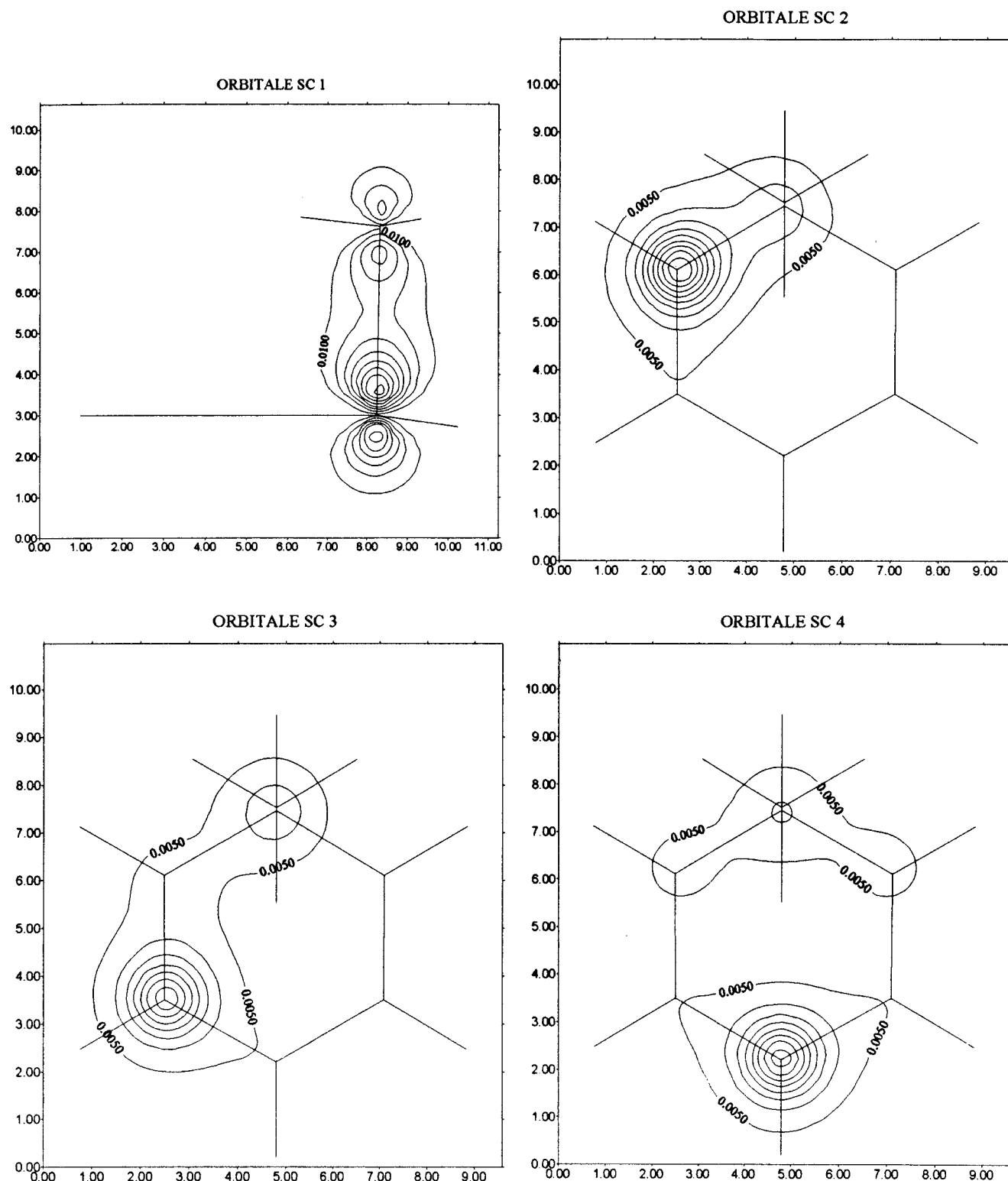


Figure 6. SC(2) solution at $R = 2.45 \text{ \AA}$: contour plots of the square of the orbitals, $|\phi_i(r)|^2$. Orbitals ϕ_2 , ϕ_3 (ϕ_5 and ϕ_6 are symmetric), and ϕ_4 are plotted in a plane parallel to the ring, shifted by $0.9 \text{ au} = 0.476 \text{ \AA}$ toward the CH_3 group. Orbital ϕ_1 is plotted in the symmetry plane defined by C_4 , C_1 , and C_7 (see Figure 1 for the numbering of the atoms).

the caption for their precise definition) and the angle formed by the $\text{C}_1\text{--C}_7$ bond and the plane of the ring (Figure 3). The first illustrates the rehybridization occurring at the two reacting C atoms, from sp^2 up to $\approx 2.5 \text{ \AA}$, to sp^3 at the equilibrium geometry. It can be seen that C_1 is somewhat more reluctant than C_7 to undergo this rearrangement, the obvious explanation being that this implies the loss of aromatic conjugation on the benzene ring. Figure 3 demonstrates that the approach of CH_3^+ does not proceed along a single direction. At long range the

interaction between the electrophile and benzene is dominated by electrostatic factors: the most favorable configuration is that in which the charged CH_3^+ group sits approximately on top of the polarizable aromatic system, so that $\text{C}_4\text{C}_1\text{C}_7 < 90^\circ$. At short range, the value of this angle is instead dictated by the tetrahedral configuration of C_1 .

Table 1 and Figure 4 contain the RHF, SC, and SCVB potential energy profiles for the reacting complex, as a function of R . Between 1.75 and 2.50 \AA there are two distinct SC

solutions, to which we refer as SC(1) and SC(2). Notice that the RHF curve runs almost parallel to those of SC and SCVB; furthermore, it leads to the correct asymptotic states of the fragments (C_6H_6 and CH_3^+ ; see also below, however). This provides some *a posteriori* justification for our RHF geometry optimizations and the frozen-core approximation for the correlated wave functions.

The SC(1) curve describes the homolytic dissociation of the C_1C_7 bond, leading to $C_6H_6^+$ and CH_3 , whereas SC(2) corresponds to heterolytic dissociation, leading to C_6H_6 and CH_3^+ . For $R < 3.0$ Å, convergence to the SC(2) solution had to be forced by restricting the spin space to three spin-couplings: the two Kekulé and one of the three Dewar structures (the one with π bonds between C_1-C_4 , C_2-C_3 , and C_5-C_6).⁸ The two SC potential energy curves cross at $R \approx 2.0$ Å, which falls exactly in the range of the reaction coordinate where rehybridization of C_1 and C_7 takes place (see Figure 2). Thus, the SC wave function furnishes a simple and chemically appealing representation of the driving force behind this geometrical rearrangement. However, this last observation cannot be considered definitive, because the structural parameters plotted in Figure 2 reflect only the behavior of the RHF wave function.

Figure 5 contains plots of the optimized SC(1) orbitals, at $R = 2.45$ Å. Even at such a large C_1-C_7 distance, the SC(1) wave function is still strikingly close to the SC solution at equilibrium (see ref 1 for the orbitals of the benzenium ion, $C_6H_7^+$). Four of the orbitals (ϕ_2 , ϕ_3 , ϕ_5 , and ϕ_6) make up the π system: they are centered on the *ortho* (C_2 and C_6) and *meta* (C_3 and C_5) positions with respect to the site of electrophilic attack, but they all spread considerably down to the *para* carbon C_1 . This provides the mechanism of charge delocalization in the Wheland intermediate.¹ Orbitals ϕ_1 and ϕ_4 form the C_1-C_7 bond: At this internuclear distance, they still have an overlap of 0.710. The Chirgwin-Coulson occupation number² of the Rumer spin function (1-4,2-3,5-6) is as large as 0.925: in other words, the electron pairs in orbitals (ϕ_1, ϕ_4), (ϕ_2, ϕ_3), and (ϕ_5, ϕ_6) are almost exactly singlet-coupled.

The SC(2) orbitals at the same value of the reaction coordinate ($R = 2.45$ Å) are plotted in Figure 6. Now all the orbitals are centered on the ring carbons, as in C_6H_6 . However, orbital ϕ_1 stretches toward C_7 , to the point of forming what could be called a "one-electron bond" between these atoms. In their turn, the remaining five orbitals all delocalize toward C_1 . Interestingly, the Dewar structure (1-4,2-3,5-6) accounts for almost 50% of the wave function (it has an occupation number of 0.477, to be compared with 0.261 for each of the two Kekulé resonance structures).

Some important insight into nature of, and the reasons for, the disappearance of the SC(1) and the SC(2) solutions (for $R > 2.50$ Å and $R < 1.75$ Å, respectively) comes from Figure 7. Here we have plotted the lowest eigenvalue of the second derivative matrix (the Hessian) of the two SC energies with respect to the wave function parameters (*i.e.*, the orbital and spin-coupling coefficients; these derivatives should not be confused with those with respect to the nuclear coordinates, which determine the vibrational spectrum). The plots are limited to the range of the R coordinate where both solutions are present. The eigenvalues are always positive, as is required by the minimum condition for a stationary point.⁹ However, by extrapolating each curve beyond the limit of stability of the corresponding SC solution, it can be seen that this eigenvalue first becomes zero and then negative. Thus, around $R = 1.75$ Å there is an important change in the nature of the SC(2) solution, which turns from a minimum into a saddle point in

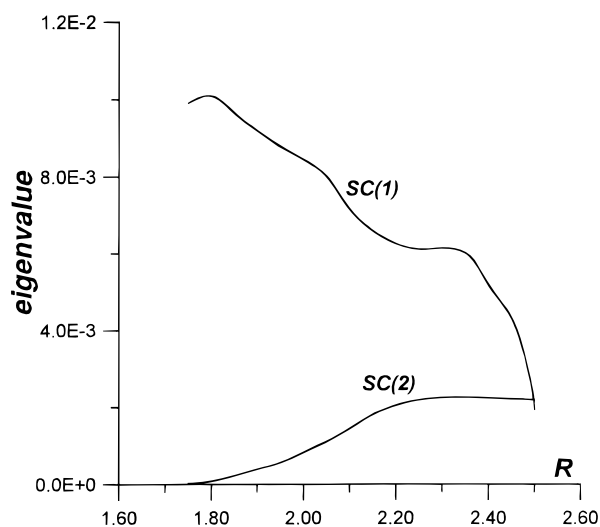


Figure 7. Lowest eigenvalues of the Hessian for the SC(1) and SC(2) solutions, as a function of R (in Å). The Hessian is the matrix of the second derivatives of the SC energy with respect to the orbital and spin-coupling coefficients. The bends on the SC(1) curve at $R \approx 1.8$, 2.0, and 2.3 Å correspond to "avoided crossings" between the first and the second (not shown) eigenvalue of the Hessian.

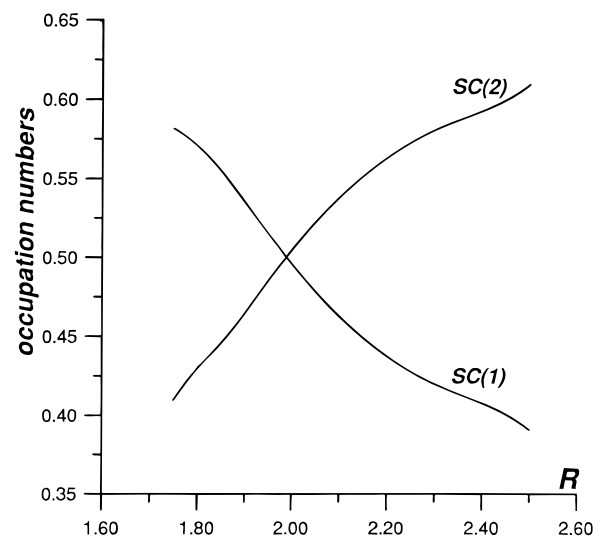


Figure 8. SCVB calculation: occupation numbers for the two orbital configurations. Each curve is the sum of the Chirgwin-Coulson occupation numbers² of the five SCVB structures associated with the SC(1) or the SC(2) configurations. The sum of the occupation numbers is equal to unity.

the SC parameter space, and similarly for the SC(1) solution at large R values.

Mixing of the SC(1) and SC(2) configurations through a nonorthogonal CI produces our SCVB wave function which, when the different allowed spin functions are included, gives rise to 10 VB structures or nonorthogonal "configuration state functions".² The lowest root of the secular problem represents the ground state of the system, whose energy is given in Table 1 and Figure 4. By the variational principle, this is obviously lower than either the SC(1) or SC(2) energies. Figure 8 shows how the nature of the SCVB wave function changes along the reaction coordinate: to the right of the crossing ($R > 2.0$ Å) the SC(2) configuration has the greatest Chirgwin-Coulson occupation number,² whereas to the left of it ($R < 2.0$ Å) it is the SC(1) configuration that dominates the wave function. Hence, the SCVB method provides a picture of the reaction in terms of an "avoided crossing" between different valence bond states.¹² We shall return to this point in the concluding section.

A final observation concerns the asymptotic states of the reacting fragments. Data from *gas-phase* photoionization spectroscopy show that in the $R \rightarrow \infty$ limit the $C_6H_6 + CH_3^+$ structure is slightly higher in energy than $C_6H_6^+ + CH_3$ (by 0.596 eV¹⁰). However, there is no trace of this in our calculations at large C_1-C_7 distances: the SC(1) solution disappears for $R > 2.50$ Å.¹¹ Instead, at large R values we only obtain the SC(2)-type solution, with heterolytic dissociation of the C_1-C_7 bond. One possible reason is that the closed-shell RHF wave function dissociates into two closed-shell fragments, so that the resulting molecular geometries and frozen-core orbitals tend to favor the same kind of dissociation. Furthermore, the single-configuration SC wave function is incapable of describing properly the electronic structure of the benzene cation, which is orbitally degenerate. Although unsatisfactory from a purely theoretical point of view, this state of affairs is not totally unwelcome from a more pragmatic one, since (i) it is the reaction between C_6H_6 and CH_3^+ that interests us, rather than that between $C_6H_6^+$ and CH_3 , and (ii) taking into account solvent effects, the correct ground state of the system at large R values would actually correspond to the SC(2)-type wave function: being smaller, but carrying the same charge, the CH_3^+ cation has a much more negative solvation free energy than either the $C_6H_6^+$ cation or the $C_6H_6CH_3^+$ intermediate.

Conclusions

We have presented spin-coupled valence bond results on the reaction pathway for a model aromatic electrophilic substitution reaction, involving the addition of a methyl cation to benzene. Optimization of the electronic wave function for the reactants and for the product (the Wheland intermediate) each leads to a single SC solution: at long range this corresponds to C_6H_6 and CH_3^+ , whereas at equilibrium the positive charge is almost completely localized on the π system of the ring, as expected.³ These two SC solutions are *qualitatively* different, so that one orbital configuration does not transform continuously into the other as the complex geometry evolves from reactants to product. Instead, there is a range of nuclear geometries where both types of solution are present and the corresponding potential energy curves cross each other. A qualitatively correct description of the complex formation is obtained by taking a linear combination of these SC solutions, in other words by constructing a two-configuration SCVB wave function; this switches continuously from one to the other configuration in the neighborhood of the crossing point.

There is a strong similarity between the present picture and the multistate VB models¹² that have been used for the rationalization of a variety of organic reaction paths. Typically, these models attempt to explain the presence as well as the height and position of an energy barrier in terms of an avoided crossing between a “repulsive” and an “attractive” VB state. There is an important difference, however. Within a semiempirical framework the VB states of the fragments are generally *assumed* to be strictly diabatic (*i.e.*, they are insensitive to changes in the nuclear geometry). The calculated diabatic potential energy curves and coupling matrix elements are generally rescaled or adjusted so as to fit the results to a set of experimental data or high-level *ab initio* calculations.¹² Here instead the building blocks of the SCVB wave function are the SC configurations, which are fully reoptimized for each value of the reaction coordinate.² A semidiabatic or “breathing orbitals” approach has also been implemented for *ab initio* VB wave functions:¹³ there is a distinct configuration representing each asymptotic state of the fragments, while the reacting

orbitals are partially relaxed at each nuclear geometry. Thus, it is generally agreed that giving up the purely diabatic picture is unavoidable within an *ab initio* VB description, if the number of configurations is to be kept to a minimum so as to ensure the interpretability of the wave function.

Ten years ago, application of SC theory demonstrated that the best single-configuration description of the π electron system of benzene is in terms of slightly deformed localized orbitals.¹⁴ The present and our previous¹ calculations show that this is not necessarily in contrast with much empirical evidence, which requires a certain degree of electron delocalization in order to explain the reactivity of this and other aromatic systems:³ the SC orbitals are highly polarizable and are ready to undergo considerable deformation in a changing environment, as for example when an electrophile approaches benzene. Moreover, a simple, transferable, and consistent pattern in the way this deformation occurs is starting to emerge: notice for example the striking similarity between the (ϕ_2, ϕ_3) orbital pairs of the SC(1) and SC(2) solutions, in Figures 5 and 6.

One important feature of our potential energy curves is the absence of a barrier (transition state) along the reaction coordinate. This is at odds with the fact that the insertion of the electrophile onto the aromatic system is generally the rate-limiting step of electrophilic substitution reactions.³ The reason for this discrepancy can be traced to our choice of the model system: the “bare” CH_3^+ cation is too strong an acid. We are planning to carry out calculations on a more realistic electrophile such as CH_3X , where X^- is a suitable leaving group (such as Cl^- in the presence of $AlCl_3$):



It will also be important to model solvent effects, for example by means of a continuum dielectric description.¹⁵

Despite some limitations, there are important methodological lessons to be learned from this study. The present SCVB approach is only applicable in a limited range of nuclear geometries, in which two distinct single-configuration SC solutions coexist. A consistent description of the whole pathway for the electrophilic substitution reaction is likely to require the adoption of a fully optimized multiconfiguration SC wave function,^{13,16} or in any case a more refined treatment of correlation effects using a larger number of conventional SCVB configurations.² We have also demonstrated that local (as opposed to absolute) minima of the SC energy can be given a chemically transparent VB-style interpretation. These minima are somewhat connected to the “breathing orbital” configurations introduced by Hiberty *et al.* and Shaik *et al.*¹³ In connection with Figure 7, it is even possible to speculate that saddle points in the SC parameter space would provide a compact and chemically appealing description of the excited states of these or other systems. Following earlier studies of the Hartree–Fock stability problem,¹⁷ a systematic investigation of the nature of the stationary points of the SC wave function should prove fruitful and instructive.

Acknowledgment. The authors thank Dr. Maurizio Sironi for computational assistance.

References and Notes

- (1) Raos, G.; Gerratt, J.; Karadakov, P. B.; Cooper, D. L.; Raimondi, M. *J. Chem. Soc., Faraday Trans.* **1995**, *91*, 4011.
- (2) (a) Cooper, D. L.; Gerratt, J.; Raimondi, M. *Adv. Chem. Phys.* **1987**, *69*, 319. (b) Cooper, D. L.; Gerratt, J.; Raimondi, M. *Int. Rev. Phys. Chem.* **1988**, *7*, 59. (c) Gerratt, J.; Cooper, D. L.; Raimondi, M. In *Valence Bond Theory and Chemical Structure*; Klein, D. J., Trinajstić, N., Eds.; Elsevier:

Amsterdam, 1990. (d) Cooper, D. L.; Gerratt, J.; Raimondi, M. *Chem. Rev.* **1991**, *91*, 929. (e) Karadakov, P. B.; Gerratt, J.; Cooper, D. L.; Raimondi, M. *J. Chem. Phys.* **1992**, *97*, 7637.

(3) (a) Streitwieser, A., Jr.; Heathcock, C. H. *Introduction to Organic Chemistry*, 3rd ed.; Macmillan Publishing Co.: New York, 1985. (b) Carey, F. A.; Sundberg, R. J. *Advanced Organic Chemistry, Part A*, 3rd ed.; Plenum Press: New York, 1990.

(4) Astorri, L. Tesi di Laurea, Università di Milano, 1995.

(5) Hehre, W. J.; Radom, L.; Schleyer, P. v. R.; Pople, J. A. *Ab Initio Molecular Orbital Theory*; Wiley: New York, 1986.

(6) Guest, M. F.; Sherwood, P. *GAMESS-UK User's Guide and Reference Manual*, Revision B.0; SERC Daresbury Laboratory: U.K., 1992.

(7) Pipek, J.; Mezey, P. G. *J. Chem. Phys.* **1989**, *90*, 4916.

(8) We believe that two excluded spin-coupling modes would play in any case a very minor role. At $R = 3.00 \text{ \AA}$ we obtained both the full-spin and the spin-restricted SC(2) solutions, the results being indistinguishable on the scale of the plot ($\Delta E = 2.6 \times 10^{-4} E_h$; see Table 1). Giving up orbital optimization and obtaining the coefficients of the two neglected spin-couplings by solving a simple secular problem over the five SC(2) structures, these always turn out to be very small (for example, at $R = 1.80 \text{ \AA}$ their Chirgwin–Coulson occupation numbers² are equal to 0.0116).

(9) The minimum of a function of several variables satisfies two conditions: the gradient vector is zero and all eigenvalues of the second

derivative matrix are greater than zero (the Hessian is positive definite). At a saddle point, the gradient is zero and the Hessian has one negative eigenvalue.

(10) Herzberg, G. *Molecular Spectra and Molecular Structure. III. Electronic Spectra and Electronic Structure of Polyatomic Molecules*; Van Nostrand Reinhold: New York, 1966.

(11) The domain of existence of the SC(1)-type wave function can actually be stretched up to 3.0 \AA by keeping a single mode of coupling of the electron spins, namely, the "perfect pairing" one.

(12) (a) Pross, A.; Shaik, S. S. *Acc. Chem. Res.* **1983**, *16*, 363. (b) Bernardi, F.; Olivucci, M.; Robb, M. A. *Acc. Chem. Res.* **1990**, *23*, 405. (c) Cooper, D. L.; Robb, M. A.; Williams, I. H. *Chem. Br.* **1990**, 1085. (d) Åqvist, J.; Warshel, A. *Chem. Rev.* **1993**, *93*, 2523.

(13) (a) Hiberty, P. C.; Humbel, S.; Byrman, C. P.; van Lenthe, J. H. *J. Chem. Phys.* **1994**, *101*, 5969. (b) Shaik, S.; Shurki, A.; Danovich, D.; Hiberty, P. C. *J. Am. Chem. Soc.* **1996**, *118*, 666.

(14) Cooper, D. L.; Gerratt, J.; Raimondi, M. *Nature (London)* **1986**, *323*, 699.

(15) Tomasi, J.; Persico, M. *Chem. Rev.* **1994**, *94*, 2027.

(16) (a) Pyper, N. C.; Gerratt, J. *Proc. R. Soc. London* **1977**, *A335*, 407.

(b) Penotti, F. *Int. J. Quantum Chem.* **1993**, *46*, 535.

(17) (a) Čížek, J.; Paldus, J. *J. Chem. Phys.* **1967**, *47*, 3976. (b) Fukutome, H. *Int. J. Quantum Chem.* **1981**, *20*, 955.